DEVELOPING A FLEXIBLE THERMAL PROTECTION SYSTEM FOR MARS ENTRY: THERMAL DESIGN AND TESTING

Alan Flinton[1], James Merrifield[1], Emma Johnstone[1], Thomas Hancock[2]
John Underwood[2], J. Stephen Lingard[2], Erhard Kaschnitz[3], Thorn Schleutker[4]
Heiko Ritter[5]

[1]Fluid Gravity Engineering Ltd, Emsworth, Hampshire, United Kingdom; [2]Vorticity Ltd, Chalgrove, Oxfordshire, United Kingdom; [3]ÖGI - Österreichisches Gießerei-Institut, Leoben, Austria; [4]German Aerospace Center (DLR), Cologne, Germany; [5]European Space Research and Technology Centre (ESTEC), Noordwijk, Netherlands

ABSTRACT

Flexible Thermal Protection Systems (FTPS) are a key technology needed to enable novel inflatable and deployable aerodynamic decelerators. A development campaign is underway to raise the European FTPS technology readiness level from 2 to 3, advancing design and test capability. An FTPS suitable for a reference Mars landing mission is being designed. The FTPS has three functional layers: outer layers of Nextel 440 BF-20 fabric; insulation layers of SIGRATHERM GFA5 graphite felt and Pyrogel XTE aerogel; and a silicone-coated Kevlar fabric gas barrier.

The density, specific heat capacity and thermal diffusivity of candidate materials was measured. Results were then used in thermal simulations to define a baseline layup. The layup thermal conductance was assessed in thermocouple-instrumented layup tests. Layups including joints were also tested and found not to have significantly different conductance. Layup test thermal simulations showed good agreement with the experimental data. Future work will include arc-jet tests and thermal model optimisation.

Index Terms— Flexible Thermal Protection System, Material Characterisation, Thermal Design

1. INTRODUCTION

Flexible Thermal Protection Systems (FTPS) are a key technology needed to enable the potential performance advantages of inflatable and deployable decelerators. By using inflatable or deployable hypersonic decelerators, heavier payloads and/or higher altitude landing sites can be achieved on future Mars missions [1]. This is because the technology allows aeroshells to be larger than the dimensions of the launcher fairing.

To improve the European capability for FTPS design and testing, a candidate FTPS is being developed. It is being designed for integration into a deployable and/or inflatable heatshield system able to fulfil the requirements of a reference mission concept landing in the Martian highlands.

The FTPS concept followed in this study is based on that developed by NASA across projects including PAIDAE [2], IRVE [3], and LOFTID [4]. This design consists of three distinct functional layers, fixed on top of one another in a layup. From the surface downwards these are:

• The outer layer. This layer must be robust enough to resist the incident heat flux, surface pressure and aerodynamic shear force throughout atmospheric entry.

• The insulation layer. The insulation layer must delay the thermal pulse caused by atmospheric heating sufficiently until the heatshield can be jettisoned, keeping the underlying structure within its thermal design limits.

• The gas barrier. The gas barrier must prevent hot gases and decomposition products from damaging the underlying structure. The gas barrier must also act to hold the insulation layers in place and provide a surface for attachments.

This paper reports results of the initial material thermal characterisation tests. Thermal modelling using results of the characterisation tests is shown and a baseline layup suggested. Finally, thermocouple layup tests to evaluate how the layup behaves in a representative environment are reported, providing a validation source for the thermal model.

An accompanying paper at FAR 2022 presents the reference mission, reference decelerator architecture and FTPS requirements; reports the material selection and mechanical characterization results, and describes the outcomes of manufacturing process trials.

2. REFERENCE MISSION

The reference mission is derived from the ESA TRP study “Aerothermodynamics Tools for Inflatable Hypersonic Decelerators” with a target landing zone in the Martian highlands [1]. Table 1 gives the key reference mission parameters. Through Monte-Carlo analysis with constraints on peak heat flux, deceleration and dynamic pressure, the resultant mission trajectory was bounded by a FPA of -10.4° (peak heat flux limit) and -9.94° (skip out limit).

Table 1 Reference mission parameters

Parameter	Value
Diameter	6.3 m
Ballistic coefficient	44 kg/m^3
Nose radius	3.3 m
Half-cone angle	60°
Nominal entry FPA	-10.2°
Peak heat flux	366 kW/m^2
Heat load	38 MJ/m^2
Peak dynamic pressure	1700 Pa

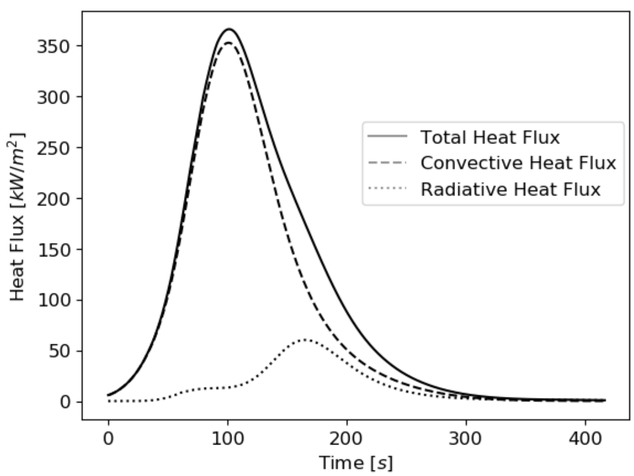

Figure 1 Reference mission heat flux, FPA of -10.2°

The heat flux was calculated using the polynomial form of the West and Brandis 2018 correlations for Martian Entry [5]. Convective multiplicative uncertainty factors of 1.2 at the stagnation point and 3.0 at the cone, and a global radiative factor of 2.0 were applied. These factors account for the effect of surface roughness, the assumption of a super-catalytic surface and general design uncertainty. The heat flux and heat load for the mission trajectory are shown in Figure 1 with convective and radiative contributions. Note that radiative heating contribution is of importance midway through the trajectory.

The reference trajectory was not altered during this study, though for testing some margin is added on the peak heat flux. If the resultant FTPS is shown to be unfeasible for the reference trajectory the study can still be considered a success. Data from this study can be taken on to other studies and trajectories more suitable to the application of FTPS technology identified and applied.

3. MATERIAL CHARACTERISATION

The comprehensive material down-selection is reported in the accompanying paper. The materials selected for further analysis were: Nextel 440 BF-20 alumina-silica-boria fibre fabric for the outer layer; SIGRATHERM GFA5 graphite felt and Pyrogel XTE silica aerogel for the insulation layer; and silicone-coated Kevlar 29 fabric for the gas barrier.

Firstly, material characterisation tests were completed to determine the thermal properties of the materials across a relevant temperature range between room temperature and 1200°C. Tests were undertaken at the Austrian Foundry Research Institute, ÖGI. Tests included were thickness and density measurements, TGA for decomposition response, DSC tests for specific heat capacity and LFA testing for thermal diffusivity. In addition, the emissivity of candidate outer layer materials was measured by ZAE Bayern.

3.1. Thickness and Density Analysis

The thickness and density of each candidate material were measured. Samples were cut from the bulk material at different positions to account for possible thickness and density variations. Thickness was measured by a micrometre screw gauge and precision callipers at several positions along each specimen. Specimen mass was measured using analytical balances. Areal density was calculated from the measured sample area and mass. From this, sample density was calculated using the measured sample thickness.

Table 2 shows the reported material thicknesses and densities. Candidate materials showed uniform properties across all samples taken for analysis, except for Pyrogel XTE. Pyrogel XTE showed significant variation in measured thickness depending on the measurement location. The material is visibly inhomogeneous, with areas of reduced thickness, especially at the edges of the roll.

Table 2 Thickness and density measurements

Material	**Thickness [mm]**	**Areal Density [g/m^3]**
Nextel 440 BF-20	0.373±0.03	491±13
SIGRATHERM GFA5	5.49±0.42	476±13
Pyrogel XTE	5.09±1.19	930±250
Silicone-coated Kevlar 29	0.230±0.015	185±4

3.2. Thermo-Gravimetric Analysis (TGA)

Thermo-Gravimetric Analysis (TGA) was performed to measure the mass loss vs temperature for the materials. The specimen was heated in an alumina pan at a constant rate of 5 K/min in an inert argon atmosphere from room temperature up to the assumed material failure temperature. During re-entry, significantly faster heating rates would be experienced

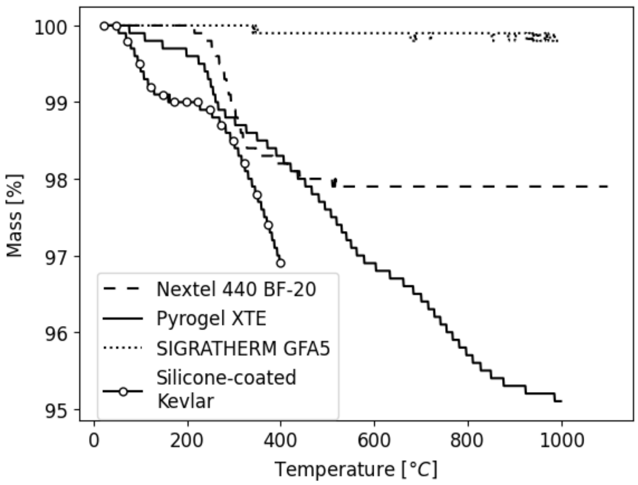

Figure 2 TGA measurements

than can be achieved in TGA, causing the onset of any reactions to occur at higher temperatures than those seen here. More representative high heating rates of the outer layer and insulation layers were achieved during the layup thermal testing reported in §5. Nevertheless, reactions captured within TGA will still be of interest at higher heating rates. The specimen holder was positioned on a precision balance, allowing the specimen mass to be measured. The temperature difference compared to a simultaneously heated reference pan was recorded, indicating the heat of possible reactions. Results are shown in Figure 2.

Nextel 440 BF-20 exhibits a mass loss of approximately 2% between 200°C and 500°C. This is due to removal of the PVA-based sizing that Nextel 440 rovings are coated with before weaving. In order to meet outgassing mission requirements, heat cleaning may be required to remove the sizing. The manufacturer 3M recommends heat cleaning via exposure to 700°C in a furnace [6], although TGA indicates that a temperature of 500°C would suffice.

SIGRATHERM GFA5 showed negligible mass loss up to 1000°C (less than 0.2%). Stability is expected up to 2000°C as reported by the manufacturer [7]; this significantly exceeds the maximum insulation layer design temperature (1500°C). The negligible mass loss indicates that negligible water vapour is absorbed by the graphite felt. As a result, thermal modelling of SIGRATHERM GFA5 need not account for the heat of thermal decomposition, provided that no significant oxidation occurs in the Martian re-entry environment.

Pyrogel XTE showed continual mass loss with increasing temperature. Variability was also seen between specimens, likely because of the inhomogeneity seen in the bulk material. One endothermic peak during decomposition

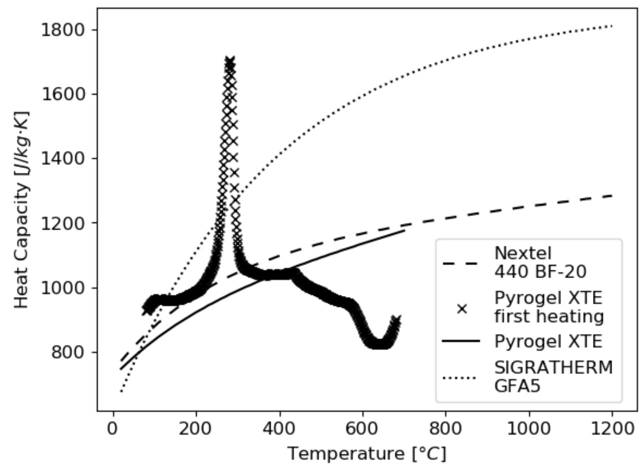

Figure 3 Specific heat capacity measurements

is visible, corresponding to the short period of increased mass loss rate between 200°C and 300°C. This decomposition effect must be included during thermal modelling.

Silicone-coated Kevlar 29 saw approximately a 1% reduction in mass between room temperature and 150°C. Water loss is the most likely explanation for this reduction as the material samples were not dried before testing; this agrees with the manufacturer data [8]. Progressive mass loss begins shortly after 200°C. This corresponds to the thermal degradation of the silicone and underlying Kevlar. The TGA heating rate is much slower than expected during use and as a result the onset temperature of degradation is likely to be higher for greater heating rates. As such a maximum design temperature of 200°C for the gas barrier layer will give a good performance margin.

3.3. Specific Heat Analysis (DSC)

Differential Scanning Calorimetry (DSC) measurements were performed to determine the specific heat capacity with temperature for the candidate materials. Specimens were heated and cooled three times at a rate of 20°C/min between room temperature and 1200°C (600°C for Pyrogel XTE). The testing was conducted in an argon atmosphere.

The results of the DSC analysis are shown in Figure 3 for the outer layer and insulation layer materials. Only Pyrogel XTE showed signs of reactions occurring, with an endothermic reaction at approximately 260°C and exothermic reactions at temperatures up to 700°C during the first heating sequence. On subsequent heating and cooling cycles the Pyrogel XTE showed no heat of reaction. These temperatures align with the temperatures at which high mass loss rates were exhibited in the TGA testing.

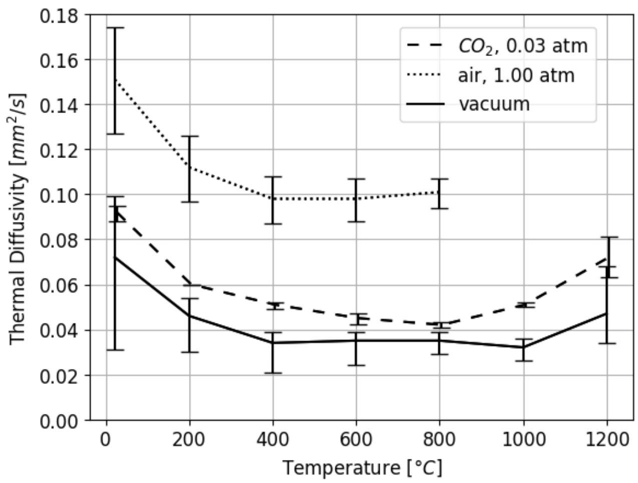

Figure 4 Thermal diffusivity measurements for Nextel 440 BF-20. Minimum and maximum values are shown by error-bar bounds

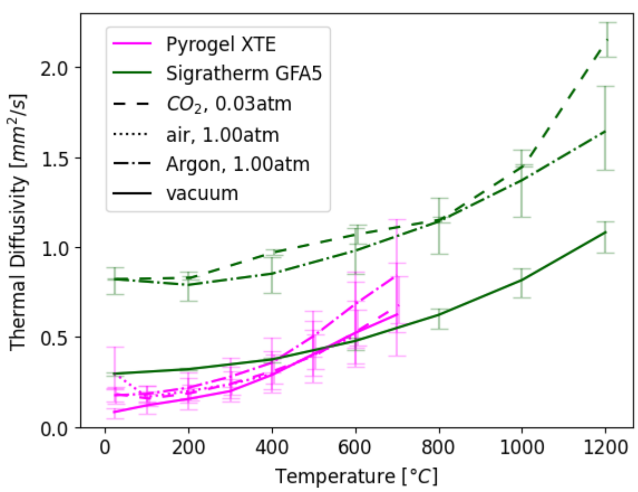

Figure 5 Thermal diffusivity measurements for SIGRATHERM GFA5 and Pyrogel XTE. Minimum and maximum values shown by error-bar bounds

3.4. Thermal Diffusivity Analysis on Materials (LFA)

Thermal diffusivity was measured using Laser Flash Analysis (LFA) from room temperature up to the material temperature limit. Measurements were taken in various atmospheres: vacuum, air at 1 atm, argon (inert) at 1 atm, and CO_2 (Mars) at 0.03 atm. All measurements had a coverage factor of 2 (95.4% confidence).

LFA results for Nextel 440 BF-20 are shown in Figure 4. The measured thermal diffusivity values varied with the ambient atmosphere. Approximately a 25% increase is seen when moving from a vacuum to a CO_2 environment. Moving from a CO_2 environment to air is shown to result in a factor of two increase in the thermal diffusivity. The Nextel 440 BF-20 values in air are similar to those published by NASA for Nextel 440 tested in N_2 between pressures of 10 mbar up to 100 mbar [9].

LFA results for the insulation layer materials are shown in Figure 5. General trends with temperature were consistent across atmospheres and materials. Pyrogel XTE has lower thermal diffusivity values compared to SIGRATHERM GFA5, especially in a CO_2 environment. From a thermal perspective, Pyrogel XTE is the leading insulation layer candidate.

SIGRATHERM GFA5 thermal diffusivity is shown to be strongly dependent on the atmospheric composition and pressure, due to the high porosity of the material. Pyrogel XTE showed no such dependency, due to its low porosity. However, Pyrogel XTE showed a much larger variation between specimens, again highlighting the inhomogeneity of the material.

3.5. Thermal Diffusivity Analysis on Layups (LFA)

LFA tests were also carried out to assess the thermal diffusivity of stacked samples as well as on SIGRATHERM GFA5 at two levels of compression.

Compression was shown to have little effect on the thermal diffusivity of the SIGRATHERM GFA per unit thickness, for both a single layer and when combined with two layers of Nextel 440 BF-20. The layups with a larger thickness had a large amount of experimental error reported, particularly above 600°C. Due to the higher thickness the back-face temperature signal was unclear, as it could not penetrate well through the layup despite being run at maximum power. It is recommended that LFA on thick layup configurations is not the best characterisation method.

3.6. Emissivity Analysis

The spectral emittance of the outer layer material was determined via experiments undertaken by ZAE Bayern. The normal and hemispherical thermal emittance were found to be 0.37±0.02 and 0.36±0.02 respectively within the uncertainty bounds of one another, indicating a Lambertian surface. The emissivity also showed a strong dependency on wavelength, suggesting that different emissivity values need to be used in thermal modelling, and when interpreting pyrometry measurements from future arc-jet tests.

4. INITIAL THERMAL ANALYSIS AND DESIGN

After the initial phase of material characterisation was completed, thermal models were developed to assess candidate layup solutions. The focus of this phase of thermal analysis was to identify a combination of insulation layer materials such that the limit temperatures of 650°C for Pyrogel XTE and 200°C at the back-face were not exceeded. Due to the limit temperature of Pyrogel XTE, it was decided that one or more layers of SIGRATHERM GFA5 will be placed on top of the Pyrogel XTE layer as insulation. Two outer layers of Nextel 440 BF-20 were selected to provide redundancy and increased outer layer strength; a single gas barrier layer was judged sufficient. The solution of choice would be the most flexible, lowest mass layup meeting the limit temperature constraints.

MABLE, FGE's 3D multi-physics code, was used to create 1D models of the FTPS layup thermal response. The surface conditions used were representative of the reference mission trajectory described in §2. The material geometry and properties used the mean values from the results of the material characterisation tests in CO_2 (air if CO_2 data was not measured). A decomposition model was constructed for Pyrogel XTE for which the virgin heat of formation was set to -60 kJ/kg. The initial temperature of the layup was set to -50°C, the backface was set as an adiabatic boundary.

The optimal layup configuration was found to be 2 layers of Nextel 440-BF-20, 2 layers of SIGRATHERM GFA5, 3 layers of Pyrogel XTE and 1 layer of silicone-coated Kevlar. This "optimal" layup was taken forward to the layup thermal testing as the baseline configuration, with another layup with only two layers of Pyrogel XTE taken as a secondary layup of interest.

The superior insulating properties of Pyrogel XTE compared to SIGRATHERM GFA5 are evident from the thermal analysis. When each material is used exclusively as an insulator four layers of Pyrogel XTE are required to meet the limit temperatures, whereas seven layers of SIGRATHERM GFA5 are required.

5. LAYUP THERMAL TESTING

Thermal layup testing was carried out by ÖGI in which a graphite crucible containing solidifying liquid copper at 1100°C was placed on top of a 120 mm square layup sample. The crucible imparted a thermal load on the FTPS layup front face while rigid insulation was present at the back face. Each sample was instrumented with eight thermocouples placed between the layers. Thermocouples were folded in 66 µm thick copper tape to ensure good thermal contact.

5.1. Test Matrix

The test matrix is shown in Table 4. The initial layup tested is that of the baseline configuration followed by a repeat. Testing with joints present in the outer and insulation layers then follows. Finally, the effect of compression upon a SIGRATHERM GFA5 only layup was assessed.

Pre-test simulation indicated that the central 50 mm square of the sample would have a low in-plane variation in temperature of less than 20°C, with edge effects expected only outside of this central core. Thermocouples were placed mainly in the centre of the specimen; some thermocouples were placed off centre to validate the hypothesis that temperature variation in the core region is low. Thermocouple placement within layers will be outlined in the later analysis section.

5.2. Results and Analysis

Figure 7a shows the thermocouple temperatures for tests 1 and 2, which were identical baseline configuration layups. Good agreement was seen between tests for corresponding thermocouples below the Nextel, Sigratherm and at the back-face. Significantly more variation was measured by the thermocouples contacting the Pyrogel XTE layers. This variation is due to the inhomogeneous nature of Pyrogel XTE as seen in the material characterisation data (§3).

Evidence of moisture evaporation is seen between 50°C and 90°C for thermocouples bordering the Pyrogel XTE. The temperature increase is mitigated within this region as energy goes into the evaporation of residual moisture. From 450°C to 500°C a rise in the rate of temperature increase suggests decomposition and heat release from the Pyrogel XTE. This temperature range is higher than that seen in the TGA and DSC analysis, due to the increased heating rate.

The inclusion of joints leads to no significant increased conduction through layers, as shown in Figure 7b. This suggests the joint threads do not act as conduction paths along which heat can travel. The joints tested are described in the accompanying paper.

Good repeatability was seen between tests 9, 10 and 12, Figure 7c, suggesting compression and inclusion of joints does not significantly alter the thermal properties of SIGRATHERM GFA5. Good agreement is also seen between tests 9, 10 and the initial heating phase of test 11. For test 11 the crucible was left in the furnace longer pre-test and as such the surface temperature remained higher for longer. This grouping of tests also highlights the homogeneity of SIGRATHERM compared to Pyrogel XTE.

The backup configuration resulted in a slightly higher back-face temperature compared to the baseline configuration as shown in Figure 7d. One thermocouple at the Sigratherm-Pyrogel interface was located outside of the central core and exhibits a slightly lower temperature showing the expected edge cooling effect.

Table 3 Test matrix for thermal layup tests

Layup Key: N=Nextel 440 BF-20, S=SIGRATHERM GFA5, P=Pyrogel XTE, K=Silicone-coated Kevlar

ID	Layup	Joints	Compression	Notes
1	2N-2S-3P-1K	No	2 mm (7%)	Baseline layup
2	Repeat of test 1			
3	2N-2S-3P-1K	Double felled seam in upper Nextel layer	2 mm (7%)	Assessment of joint in Nextel
4	2N-2S-2P-1N	No	2 mm (7%)	Backup layup
5	2N-2S-3P-1K	2nd Sigratherm and Pyrogel layers split, edges laced together	2 mm (7%)	Assessment of joint in insulation layer
6	2N-2S-3P-1K	Quilting through entire outer layer and insulation layers	2 mm (7%)	Assessment of joints through layup
7	1N-2S-3P-1K	Double felled seam in second Nextel layer	2 mm (7%)	Assessment of joint in Nextel
8	Repeat of test 5			
9	2N-5S-1K	No	2 mm (7%)	Sigratherm only
10	2N-5S-1K	No	3.8 mm (14%)	Sigratherm only, assessment of the effect of compression
11	2N-5S-1K	No	5.5 mm (20%)	
12	2N-5S-1K	Joints in 2nd and 4th Sigratherm layers	5.5 mm (20%)	

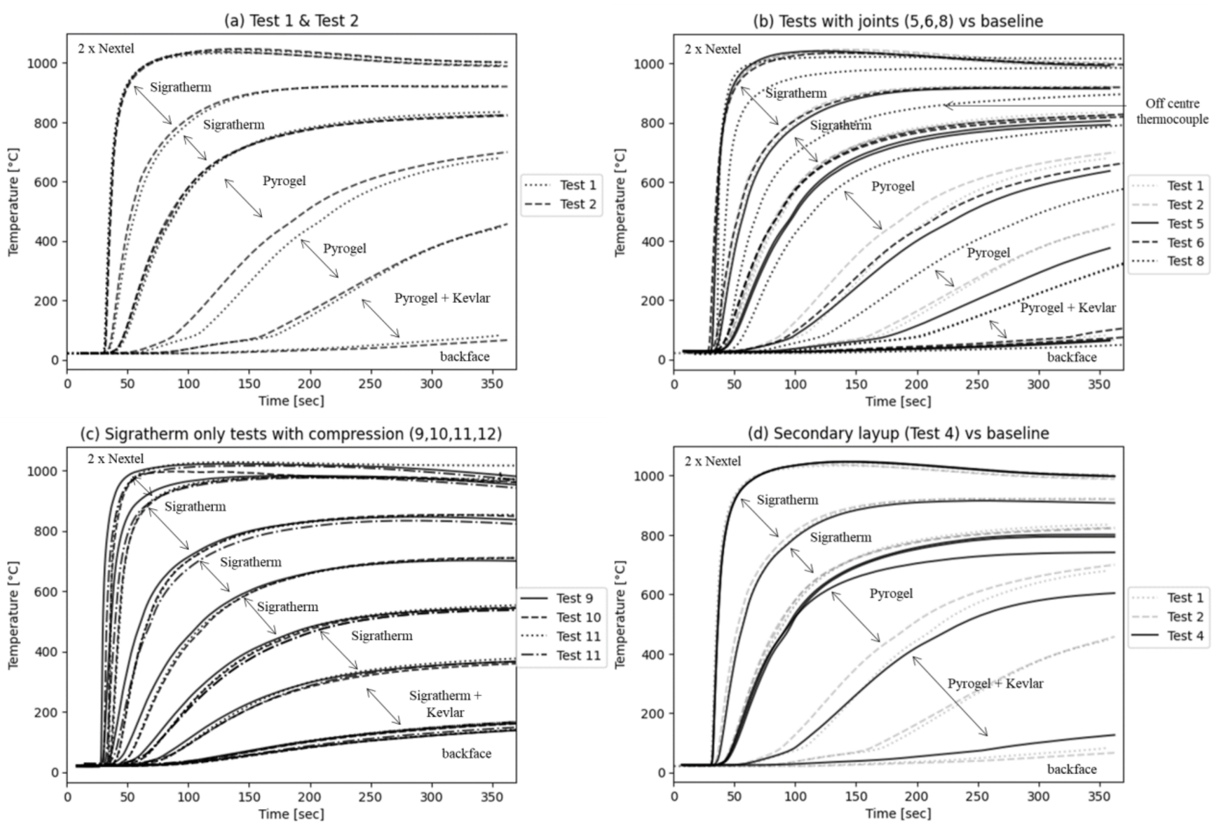

Figure 6 Results of thermal layup tests

6. NUMERICAL REBUILDS

6.1. Setup

1D MABLE rebuilds of the test layups were performed. The rebuilds did not model joints; the focus was to achieve good characterisation of the bulk materials.

The material properties for the MABLE rebuilds were taken from the material characterisation data shown in §3. Minimum and maximum values for thermal conductivity were taken to show a gauge of the current suitability of the MABLE material model. The environment was taken to be air. Thermal diffusivity was adjusted with the material compression used, assuming thermal diffusivity ratio to be proportional to the square of the material thickness ratio. The back-face was modelled as 5 cm thick furan-bonded sand. Perfect thermal contact was assumed between all layers. For tests 1 to 6, the surface temperature was assumed to be the melting temperature of copper, 1100°C, for tests 6 to 12 the surface temperature was set to that of the available surface thermocouple.

6.2. Results and Analysis

The in-depth MABLE temperatures compared to the available thermocouple data from tests 1 and 2 are shown in Figure 7. The experimental data falls within the bounds of the MABLE model during the initial temperature rise phase; after this there is a small difference. Data from test 7 onwards (with a thermocouple present at the surface) suggest that the surface temperature is not a constant 1100°C, which will lead to a deviation between simulation and experiment. A wider predicted temperature range seen at the depth of the Pyrogel XTE compared to the SIGRATHERM GFA5 is due to the greater variability of the Pyrogel XTE properties.

Figure 8 shows results from a thermal model of test 8 compared to experimental data. The surface thermocouple was used as the surface temperature boundary condition for this simulation. The experimental temperature profiles are within the bounds of the MABLE model from the initial heating phase through the cooling period. The MABLE model using the minimum conductivity values showed good agreement. The variability in Pyrogel XTE is again evident.

A rebuild of test 11 is shown in Figure 9. Pyrogel XTE was not present for this configuration allowing the test to be free from the high variability induced by Pyrogel XTE. A constant deviation is seen between the MABLE data and the experimental data from the very top layer down throughout. This suggests the Nextel 440 BF-20 material model could be further improved, as well as considering other factors such as contact resistance. The MABLE case was repeated using the second shallowest thermocouple as a boundary condition to eliminate this deviation at the surface; the resulting agreement between the experimental results and the MABLE data is significantly improved. This gives confidence in the SIGRATHERM GFA5 model used.

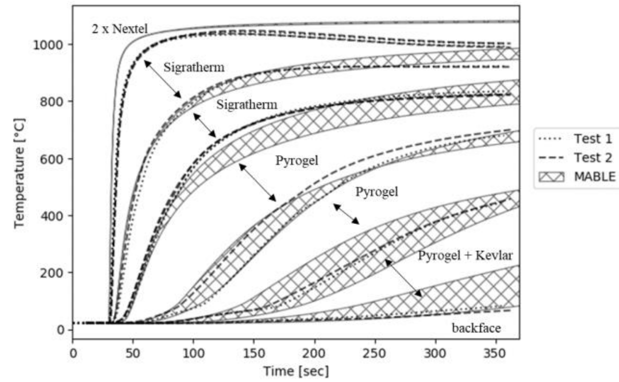

Figure 7 Thermocouple results from tests 1 & 2 compared to MABLE rebuild

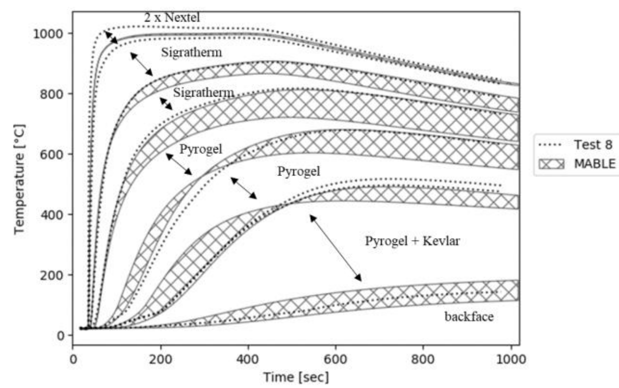

Figure 8 Thermocouple results from test 8 compared to MABLE rebuild

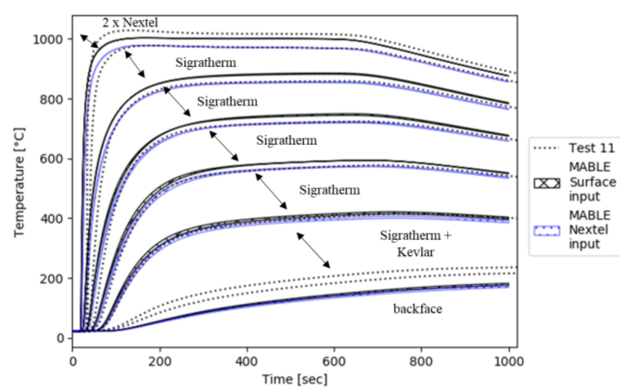

Figure 9 Thermocouple results from test 11 compared to MABLE rebuild

7. ARC-JET TESTING

The next stage of the project is arc-jet testing to be undertaken using the L2K facility at DLR Cologne.

The primary layup configuration to be evaluated will be that of 2 layers of Nextel 440 BF-20, 3 layers of SIGRATHERM GFA5, 1 layer of Pyrogel XTE and 1 layer of silicone-coated Kevlar. A reduced number of Pyrogel XTE layers will be considered to achieve an acceptable overall layup flexibility. Two configurations are to be assessed: a stagnation setup and a tangential setup, the latter allowing the effect of surface shear to be studied. A heat flux of 400 kW/m^2 will be targeted as a baseline value. A higher heat flux and load may also be targeted in later tests dependent on the results of the primary arc-jet tests. The freestream atmosphere within the arc jet will be 95% CO_2, 3% N_2 and 2% Ar by volume, representative of Mars re-entry.

The data from the arc-jet testing will show how the layup surface behaves in a representative flow environment, and design limits inherent in the Nextel or joining methods may become apparent. The arc-jet tests will also provide further thermocouple data, which will be used to improve and validate the material thermal models.

8. SUMMARY AND CONCLUSIONS

Development is ongoing to increase the European understanding of the thermal capabilities of FTPS.

Thermal characterisation testing allowed materials of interest to be compared. An initial FTPS layup was suggested through development of thermal simulations using the material characterisation test data.

Experimental thermocouple layup testing was undertaken successfully. The influence of joints within the layup on in-depth temperature was shown to be minimal. Experimental data also showed the high variability in Pyrogel XTE properties compared to the other materials considered.

Thermal rebuilds of the layup tests were undertaken, which yielded good agreement with the experimental data. Simulation of the Sigratherm GFA5 only insulation layup gave particularly good agreement showing confidence in the material model used.

The next stage of the study, an arc-jet campaign, is currently underway, which will allow further characterisation of the FTPS solutions and optimisation of the thermal model.

This paper details only the thermal design considerations of the overall project. When considering all aspects of the FTPS, trade-offs between the thermal requirements and structural and mission requirements must be made, considering the knowledge gathered from complementary experimental studies reported in the accompanying paper.

9. REFERENCES

[1] J. Underwood, J. S. Lingard, J. Merrifield and E. Johnstone, "European Studies to Advance Development of Deployable and Inflatable Aerodynamic Decelerators," in *International Conference on Flight Vehicles, Aerothermodynamics and Re-Entry Missions & Engineering (FAR)*, Monopoli, 2019.

[2] J. A. Del Corso, "Thermal Analysis and Testing of Candidate Materials for PAIDAE Inflatable Aeroshell," in *20th AIAA Aerodynamic Decelerator Systems Technology Conference and Seminar*, Seattle, 2009.

[3] K. Johnson, F. Cheatwood, A. McNeil, S. Hughes, A. Korzon, J. DiNonno, M. Lindell and G. Swanson, "HIAD Advancements and Extension of Mission Applications," in *International Planetary Probe Workshop*, Laurel, MD, 2016.

[4] NASA, "Low-Earth Orbit Flight Test of an Inflatable Decelerator (LOFTID)," NASA, 2019.

[5] T. K. West IV and M. A. Brandis, "Updated Stagnation Point Aeroheating Correlations for Mars Entry," in *Joint Thermophysics and Heat Transfer Conference*, Atlanta, Georgia, 2018.

[6] 3M Advanced Materials Division, "3M™ Nextel™ Ceramic Fibers and," St. Paul, MN, 2018.

[7] SGL Carbon, "SIGRATHERM GFA," SGL Carbon, Datasheet. TDS FGA.00, 2018.

[8] DuPont, "Kevlar Aramid Fiber Technical Guide. s.l.," DuPont, Datasheet, 2017.

[9] F. Cheatwood, A. McNeil and W. Bruce, "Advanced High-Temperature Flexible TPS for Inflatable Aerodynamic Declerators," *AIAA*, pp. 2011-2510, 2011.

[10] E. Johnstone, B. Esser, A. Guelhan, S. Overent, J. Underwood and L. Ferracina, "Investigating the Response of a Flexible TPS to a High Enthalpy Environment," in *FAR*, Monopoli, Italy, 2019.